

# Helicity Amplitudes for $\mathcal{O}(\alpha_s)$ Production of $W^+W^-$ , $W^\pm Z$ , $ZZ$ , $W^\pm\gamma$ , or $Z\gamma$ Pairs at Hadron Colliders

L. Dixon<sup>1,a</sup>, Z. Kunszt<sup>2</sup> and A. Signer<sup>3</sup>

<sup>1</sup>*Stanford Linear Accelerator Center, Stanford University, Stanford, CA 94309, USA*

<sup>2</sup>*Theoretical Physics, ETH Zürich, Switzerland*

<sup>3</sup>*Theory Division, CERN, CH-1211 Geneva 23, Switzerland*

## Abstract

We present the one-loop QCD corrections to the helicity amplitudes for the processes  $q\bar{q} \rightarrow W^+W^-$ ,  $ZZ$ ,  $W^\pm Z$ ,  $W^\pm\gamma$ , or  $Z\gamma$ , including the subsequent decay of each massive vector boson into a pair of leptons. We also give the corresponding tree-level amplitudes with an additional gluon radiated off the quark line. Together, these amplitudes provide all the necessary input for the calculation of the next-to-leading order QCD corrections to the production of any electroweak vector boson pair at hadron colliders, including the full spin and decay angle correlations.

*Submitted to Nuclear Physics B*

---

<sup>a</sup>Research supported by the US Department of Energy under grant DE-AC03-76SF00515.

# 1 Introduction

With the increasing energy available at hadron colliders, electroweak gauge boson pair production becomes more and more important. Both experimental collaborations at the Tevatron, CDF [1] and D0 [2], have performed studies of pair production processes such as  $p\bar{p} \rightarrow W^+W^-, ZZ, W^\pm Z, W^\pm\gamma$ , or  $Z\gamma$ . These studies considered purely leptonic decays of the massive vector bosons in the pair, as well as decays into two jets plus leptons. Already, some events have been found above the background, in accordance with Standard Model predictions. The amount of available data will increase by roughly a factor of 20 at the upgraded Tevatron, and by a factor of 1000 once the Large Hadron Collider at CERN (LHC) starts operating. A summary of the present experimental situation and a more complete list of earlier studies can be found in [3].

These processes are quite interesting in several respects. Most of all, they can be used to measure the vector boson trilinear couplings predicted by the Standard Model [4]. Any kind of anomalous couplings, or decays of new particles into vector boson pairs, would result in deviations from these predictions. In particular, if the Higgs boson is heavy enough it will decay mainly into  $W^+W^-$  and  $ZZ$  pairs [5]. Thus, the search for Higgs bosons in the few hundred GeV mass range is intimately connected to pair production of vector bosons. A detailed understanding of these Standard Model processes is therefore mandatory.

Due to its importance, hadronic pair production of electroweak vector bosons has received a lot of attention in the literature. The tree-level cross-sections for the hadronic production of  $W^+W^-$ ,  $ZZ$ ,  $W^\pm Z$ , as well as  $W^\pm\gamma$  and  $Z\gamma$  pairs were computed long ago [6]. The one-loop ( $\mathcal{O}(\alpha_s)$ ) QCD corrections to these cross-sections have been computed in [7, 8] for  $ZZ$ , in [9, 10] for  $W^\pm Z$ , in [11, 12] for  $W^+W^-$ , and in [13, 14] for  $W^\pm\gamma$  and  $Z\gamma$ . These computations were all done with the traditional method of evaluating directly the squared amplitude through interference (cut) diagrams and evaluating the traces in  $D = 4 - 2\epsilon$  dimensions. As a consequence, the computed cross-sections were summed over all  $W$  and  $Z$  polarization states.

A more realistic treatment of these processes can be obtained by properly including the decay of the vector bosons into massless fermions. In fact, vector bosons are identified through these decay products. Thus, the comparison of theory and experiment is much easier, since cuts on the kinematics of the decay products can easily be added to the computation. As one example of the importance of decay-angle correlations, it has been proposed [15, 16] to search for the Higgs boson at the LHC in the intermediate mass range  $m_H = 155 - 180$  GeV in the channel  $H \rightarrow W^+W^- \rightarrow \ell^+\nu\ell^-\bar{\nu}$ . To reduce the continuum  $W^+W^-$  background, one can exploit [16] the anti-correlation between  $W$  helicities for the signal process, as well as the strong correlation between the  $W$  helicity and the decay lepton direction; the signal peaks when  $\ell^+$  and  $\ell^-$  are nearly collinear,  $\cos\theta_{\ell^+\ell^-} \approx 1$ , while the background is relatively flat in this variable. For such a search it is clearly important to understand as well as possible the background distributions for  $\cos\theta_{\ell^+\ell^-}$  and other kinematic variables.

In the narrow-width approximation, vector boson decay is simple to implement at the amplitude level. Because the couplings of vector bosons to fermions are spin-dependent (especially the purely left-handed  $W$  couplings), it is natural to employ the helicity method and compute amplitudes for massless external states of definite helicity. The tree-level

helicity amplitudes for massive vector-boson pair production with subsequent decay into leptons were first computed in [17]. The authors of [17] also showed that the effects of decay-angle correlations are significant.

In [18], the above two approaches were merged to get a more complete next-to-leading order treatment of vector boson pair production. In this work spin correlations were included everywhere except for the virtual contribution. Furthermore, the calculations were extended to include also non-standard triple-vector-boson couplings. However, only numerical results were presented, making it difficult to use these results in future computations.

The present paper closes this gap by presenting all helicity amplitudes required for next-to-leading order (in the strong coupling  $\alpha_s$ ) hadronic production of a vector boson pair. In particular, we give the one-loop amplitudes with a virtual gluon for the processes

$$\bar{q}q \rightarrow W^-W^+ \rightarrow (\ell\bar{\nu}) + (\bar{\ell}'\nu'), \quad (1.1)$$

$$\bar{q}q \rightarrow Z Z \rightarrow (\ell\bar{\ell}) + (\bar{\ell}'\ell'), \quad (1.2)$$

$$\bar{u}d \rightarrow W^-Z \rightarrow (\ell\bar{\nu}) + (\bar{\ell}'\ell'), \quad (1.3)$$

$$\bar{u}d \rightarrow W^-\gamma \rightarrow (\ell\bar{\nu}) + \gamma, \quad (1.4)$$

$$\bar{q}q \rightarrow Z\gamma \rightarrow (\ell\bar{\ell}) + \gamma. \quad (1.5)$$

The processes with a  $W^+Z$  or a  $W^+\gamma$  pair as intermediate state can be obtained from eq. (1.3) and eq. (1.4) by a CP transformation. The decay of the vector bosons into leptons is included in the narrow-width approximation. We also present the tree-level amplitudes for the same processes with an additional gluon radiated off the quark line. (The gluon may also appear in the initial state. The corresponding amplitudes can be obtained by crossing symmetry.) Both sets of amplitudes are needed for a complete next-to-leading order computation of the cross-sections for vector-boson pair production.

In the spinor helicity formalism [19], the tree-level amplitudes are trivial to obtain and the results are very compact. For the one-loop amplitudes, it was not necessary to do a full computation. Almost all of the terms could be extracted from one of the helicity amplitudes for the process  $e^+e^- \rightarrow q\bar{q}Q\bar{Q}$  as presented in [20], where  $q$  and  $Q$  are massless quarks of different flavor. In fact, knowledge of the ‘primitive amplitude’ (see section 2) for the subleading-in-color piece of  $e^+e^- \rightarrow q\bar{q}Q\bar{Q}$  is sufficient to obtain all one-loop amplitudes for the processes listed in eqs. (1.1)–(1.3). The amplitude for the process (1.4) can also be obtained without doing a full computation. It is sufficient to replace the  $Z$  in the process (1.3) by a virtual photon  $\gamma^*$ . Then the desired amplitude can be extracted from the collinear limit of the decay products of the virtual photon. Finally, these results allow for the construction of the amplitude for the last missing process, eq. (1.5). This last result could also be obtained from the known subleading-in-color primitive amplitude for  $e^+e^- \rightarrow q\bar{q}g$  [21, 22].

Besides their contribution to next-to-leading order pair production rates, the one-loop amplitudes also contribute, via their absorptive parts, to kinematic structures which are odd under ‘naive’ time reversal (the reversal of all momentum and spin vectors in a process). Such terms are not present at tree level; also, they are washed out if one integrates over all the leptonic decay angles. Analogous effects were considered quite some time ago, in the production of  $W + 1$  jet at hadron colliders [23].

In section 2 we exploit the results of [20] in order to obtain certain primitive amplitudes,

called  $A^a$  and  $A^b$ , which serve as building blocks for the construction of all the one-loop amplitudes for  $q\bar{q} \rightarrow W^+W^-$ ,  $ZZ$ ,  $W^\pm Z \rightarrow 4$  leptons. This construction will be performed in section 3. Section 4 is devoted to the processes with a real photon in the final state. Finally, in section 5 we compare our results to the literature [8, 10, 12, 13] and present our conclusions.

## 2 Primitive amplitudes for $W^+W^-$ , $ZZ$ , $W^\pm Z$

### 2.1 Preliminaries

It is by now standard to use the helicity method and color ordering of the amplitudes to simplify one-loop calculations in QCD (for a review see e.g. [24]). The results for the helicity amplitudes will be expressed in terms of spinor inner products,

$$\langle ij \rangle \equiv \langle k_i^- | k_j^+ \rangle, \quad [ij] \equiv \langle k_i^+ | k_j^- \rangle, \quad (2.1)$$

where  $|k_i^\pm\rangle$  is the Weyl spinor for a massless particle with momentum  $k_i$ . The spinor inner products are antisymmetric and satisfy  $\langle ij \rangle [ji] = 2k_i \cdot k_j \equiv s_{ij}$ . For later use we also define

$$\begin{aligned} \langle i|l|j \rangle &\equiv \langle k_i^- | \not{k}_l | k_j^- \rangle, \\ \langle i|lm|j \rangle &\equiv \langle k_i^- | \not{k}_l \not{k}_m | k_j^+ \rangle, \\ \langle i|(l+m)|j \rangle &\equiv \langle k_i^- | (\not{k}_l + \not{k}_m) | k_j^- \rangle, \\ \langle i|(l+m)(n+r)|j \rangle &\equiv \langle k_i^- | (\not{k}_l + \not{k}_m)(\not{k}_n + \not{k}_r) | k_j^+ \rangle, \\ [i|\dots|j] &\equiv \langle i|\dots|j \rangle \Big|_{k_{\{i,j\}}^\pm \rightarrow k_{\{i,j\}}^\mp} \end{aligned} \quad (2.2)$$

and

$$\begin{aligned} s_{ij} &\equiv (k_i + k_j)^2, & t_{ijm} &\equiv (k_i + k_j + k_m)^2, \\ \delta_{12} &\equiv s_{12} - s_{34} - s_{56}, & \delta_{34} &\equiv s_{34} - s_{12} - s_{56}, & \delta_{56} &\equiv s_{56} - s_{12} - s_{34}, \\ \Delta_3 &\equiv s_{12}^2 + s_{34}^2 + s_{56}^2 - 2s_{12}s_{34} - 2s_{12}s_{56} - 2s_{34}s_{56}. \end{aligned} \quad (2.3)$$

For all the processes  $q\bar{q} \rightarrow V_1V_2 \rightarrow 4$  leptons, where  $V_{1,2} \equiv W^\pm$  or  $Z$ , the color ordering of the amplitudes is trivial: All diagrams have the same color factor. Thus the full amplitude can be obtained by taking the one and only subamplitude (partial amplitude) and multiplying it by the overall color factor.

Still, the diagrams which contribute to  $q\bar{q} \rightarrow V_1V_2 \rightarrow 4$  leptons naturally fall into two classes, which can be distinguished by their different dependence on the electroweak coupling constants, and which therefore are separately gauge invariant. (See Fig. 1.) This decomposition is analogous to the decomposition of QCD amplitudes into primitive amplitudes [25]. The first class (diagrams  $(a_i)$  of Fig. 1) has no triple-electroweak-vector-boson vertex. There is only one such tree graph,  $(a_0)$ . We call the one-loop box graph  $(a_1)$  the ‘box-parent’ because the other one-loop graphs in this class,  $(a_{1,1}) - (a_{1,3})$ , can be obtained from  $(a_1)$  by sliding the virtual gluon line around, while leaving the electroweak vector bosons fixed.

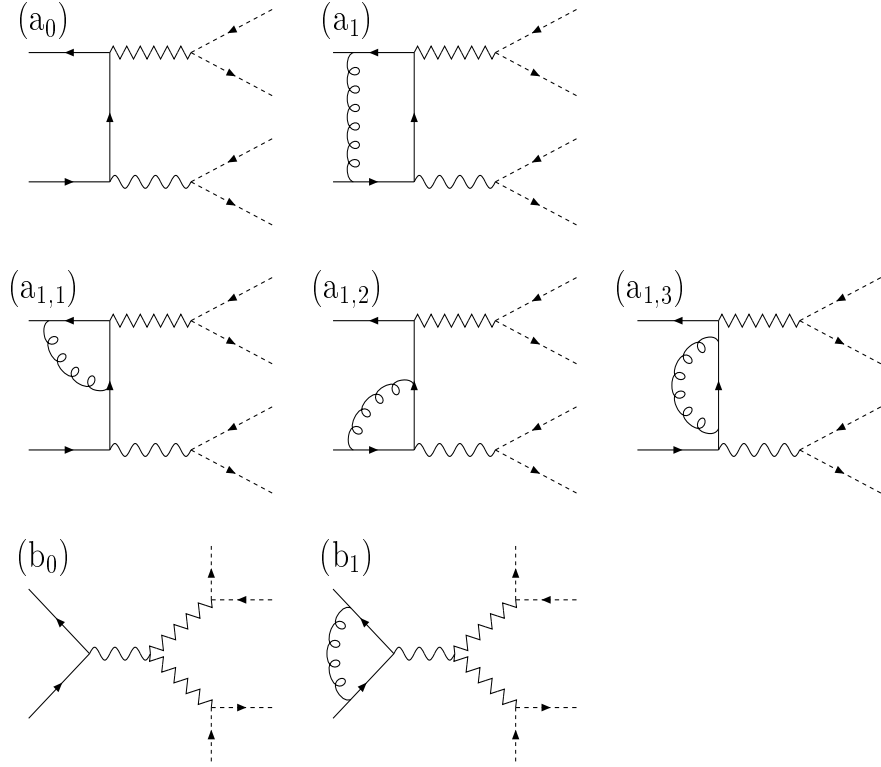


Figure 1: (a<sub>0</sub>) box-parent tree graph; (a<sub>1</sub>) box-parent one-loop graph; (a<sub>1,1</sub>) – (a<sub>1,3</sub>) additional one-loop graphs obtained from the box-parent graph; (b<sub>0</sub>) triangle-parent tree graph; (b<sub>1</sub>) triangle-parent one-loop graph. Solid (dashed) lines represent quarks (leptons). In order to distinguish the possibly different vector bosons we used zigzag and wavy lines. For the graphs b<sub>0</sub> and b<sub>1</sub> we show the diagrams for the  $W^+W^-$  intermediate state.

(Bubble graphs where a gluon dresses a massless external quark line are zero in dimensional regularization.) The tree-level primitive amplitude  $A^{\text{tree},a}$  is defined to be just the contribution of the graph (a<sub>0</sub>), omitting all coupling constant prefactors. The one-loop primitive amplitude  $A^a$  is similarly defined by the sum of graphs (a<sub>1</sub>) and (a<sub>1,1</sub>) – (a<sub>1,3</sub>). The second class (diagrams (b<sub>i</sub>) of Fig. 1) contains a three-boson vertex. In this class, there are no further graphs besides the parent graphs. These primitive amplitudes will be denoted by  $A^{\text{tree},b}$  and  $A^b$ . Because  $A^b$  consists of a single triangle diagram, it is much simpler than  $A^a$ .

We present amplitudes in the dimensional reduction [26] or four-dimensional helicity [27] variants of dimensional regularization, which are equivalent at one loop. The conversion to other variants is straightforward [28].

## 2.2 Relation to subleading-color $e^+e^- \rightarrow q\bar{q}Q\bar{Q}$ amplitude

The one-loop amplitudes for  $q\bar{q} \rightarrow V_1V_2 \rightarrow 4$  leptons can be obtained *almost* completely from the subleading-color amplitude  $A_6^{\text{sl}}(1, 2, 3, 4)$  for the process  $e^+e^- \rightarrow q\bar{q}Q\bar{Q}$ , as given

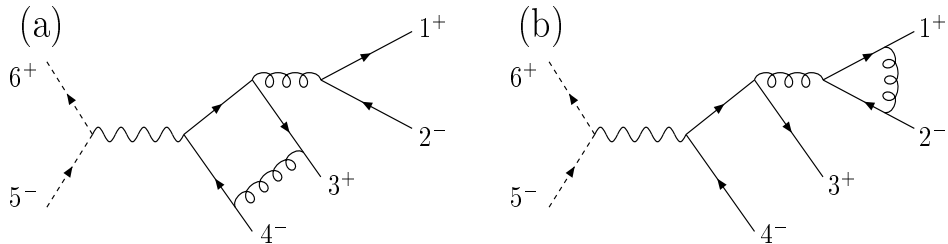


Figure 2: Parent diagrams for  $A_6^{\text{sl}}(1,2,3,4)$ , i.e. the subleading-in-color part of  $e^+e^- \rightarrow q\bar{q}Q\bar{Q}$ . Solid (dotted) lines represent quarks (electrons). Note that the labeling used in this figure and in section 2.2 corresponds to the one used in ref. [20].

in eqs. (3.16)–(3.21) of [20]<sup>1</sup>. The ‘parent’ graphs for that amplitude are shown in Fig. 2. Graph (a) is obviously very similar to corresponding box-parent graph (a<sub>1</sub>) in Fig. 1. The quark pair {1, 2} can be replaced by a lepton pair, and the virtual gluon that connects the two different quark lines can be replaced by an electroweak vector boson. The fact that the vector boson can have axial-vector as well as vector couplings, while the gluon has only vector couplings, can be accounted for in the helicity formalism simply by dressing the graphs with the appropriate left- and right-handed couplings of fermions to electroweak bosons.

If  $A_6^{\text{sl}}(1,2,3,4)$  were truly a primitive amplitude, then one would be able to get  $q\bar{q} \rightarrow V_1V_2 \rightarrow 4$  leptons from it with no further information. However, the  $A_6^{\text{sl}}(1,2,3,4)$  as given in [20] is not truly primitive, for two reasons.

Firstly, the diagrams (a) and (b) in Fig. 2 are combined together in  $A_6^{\text{sl}}(1,2,3,4)$ . However, it is no problem to remove diagram (b), because its contribution has been identified explicitly in [20] (as the terms in the second bracket in eq. (3.19) for  $V^{\text{sl}}$ ). Both diagrams (b<sub>1</sub>) of Fig. 1 and (b) of Fig. 2 are QCD vertex corrections, which evaluate to a universal factor times the corresponding tree graph. Thus the terms from diagram (b) in Fig. 2, which appeared multiplied by  $A_6^{\text{tree,sl}}$  in [20], will reappear here in  $A^b$ , multiplied instead by  $A^{\text{tree},b}$ .

Secondly, and more non-trivially, another class of graphs has also been included in  $A_6^{\text{sl}}(1,2,3,4)$  in addition to those shown in Fig. 2 — those where the quark pair {5, 6} and the lepton pair {1, 2} are exchanged. In the process  $e^+e^- \rightarrow q\bar{q}Q\bar{Q}$ , both classes of graphs have equal weight, but in  $q\bar{q} \rightarrow V_1V_2 \rightarrow 4$  leptons they do not (except for the  $ZZ$  case). The permutation that generates the ‘exchange’ terms is

$$\text{exchange:} \quad 1 \leftrightarrow 6, \quad 2 \leftrightarrow 5. \quad (2.4)$$

We need to delete the ‘exchange’ terms from the (a) terms in  $A_6^{\text{sl}}(1,2,3,4)$ . Since ‘exchange’ takes  $t_{123}$  to  $t_{124}$ , part of this deletion is easy to implement — we want to omit all terms with a cut in the  $t_{124}$  channel, for example. Also, the second term in the tree amplitude  $A_6^{\text{tree,sl}}$  in eq. (3.16) of [20] should clearly be omitted. But this is not enough. There is still

<sup>1</sup>In order to simplify the discussion at this point, we use the labeling of [20] in section 2.2. The labeling used in the rest of this paper can be obtained from it by the replacement  $\{1, 2, 3, 4, 5, 6\} \rightarrow \{5, 6, 2, 1, 3, 4\}$ .

a potential ambiguity about which terms come from the desired graphs, and which terms from the exchange graphs, in the coefficients of  $\ln(s_{12})$ ,  $\ln(s_{56})$ ,  $\ln(s_{34})$  and the three-mass triangle integral  $I_3^{3m}(s_{12}, s_{34}, s_{56})$ , as well as the rational-function terms.

Fortunately, it turns out that all of the ambiguous terms, except for the rational-function terms, *were* given in eqs. (3.20) and (3.21) of [20] as the contributions of the desired graphs, not including the exchange. The exchange that was desired for  $e^+e^- \rightarrow q\bar{q}Q\bar{Q}$  was then added explicitly, at the end of eq. (3.20). This same statement is *not* true for a second (simpler) form of  $A_6^{\text{sl}}(1, 2, 3, 4)$ , given in eqs. (12.9)–(12.12) of [22]. In that form, the exchange symmetry was used extensively to simplify the coefficients of  $\ln(s_{12})$  and  $I_3^{3m}$ , at the cost, however, of hopelessly entangling the desired graphs with their exchange. (However, we have managed to significantly simplify even the non-exchange form of these coefficients, as one may appreciate by comparing eq. (2.16) below to eq. (3.21) of [20].)

We have calculated the desired rational-function terms. We find that  $F^{\text{sl}}(1, 2, 3, 4)$  as given in eq. (3.20) of [20] is also valid for the non-exchange case, provided only that the final ‘+exchange’ instruction is dropped, and that the following rational-function terms are added to the existing terms:

$$\delta p \equiv -\frac{1}{2} \frac{1}{\langle 3|(1+2)|4\rangle} \left( \frac{[16]^2}{[12][56]} + \frac{\langle 25\rangle^2}{\langle 12\rangle\langle 56\rangle} \right) - \frac{1}{2} \frac{\langle 2|(1+3)|6\rangle\langle 5|(2+4)|1\rangle}{s_{12}s_{56}\langle 3|(1+2)|4\rangle}. \quad (2.5)$$

## 2.3 Virtual primitive amplitudes

After simplifying the coefficients of  $\ln(s_{12})$  and  $I_3^{3m}$ , we can write a fairly compact form for the required one-loop primitive amplitudes,

$$A^\alpha(1, 2, 3, 4, 5, 6), \quad \alpha = a, b. \quad (2.6)$$

In the application to the processes  $q\bar{q} \rightarrow V_1V_2 \rightarrow 4$  leptons, the quark and anti-quark will always be drawn from the set  $\{1, 2\}$ , while the leptonic decay products of a vector boson will be  $\{3, 4\}$  or  $\{5, 6\}$ . However, the exact correspondence depends on the fermion helicity; i.e., the same function will appear with various permutations of its arguments  $(1, 2, 3, 4, 5, 6)$  in section 3. The helicity assignments in eq. (2.6) are  $(1^-, 2^+, 3^-, 4^+, 5^+, 6^-)$  (when all particles are considered outgoing). For the rest of this section the arguments  $(1, 2, 3, 4, 5, 6)$  will be implicit.

First define the flip symmetry,

$$\text{flip}_1 : \quad 1 \leftrightarrow 2, \quad 3 \leftrightarrow 5, \quad 4 \leftrightarrow 6, \quad \langle ab \rangle \leftrightarrow [ab]. \quad (2.7)$$

The box-parent tree graph is given by

$$A^{\text{tree},a} = i \frac{\langle 13 \rangle [25] \langle 6|(2+5)|4 \rangle}{s_{34}s_{56}t_{134}}. \quad (2.8)$$

The triangle-parent tree graph is given by

$$A^{\text{tree},b} = \frac{i}{s_{12}s_{34}s_{56}} \left[ \langle 13 \rangle [25] \langle 6|(2+5)|4 \rangle + [24] \langle 16 \rangle \langle 3|(1+6)|5 \rangle \right], \quad (2.9)$$

in a form that agrees with [17].

At one loop, we perform a decomposition into a universal divergent piece  $V$ , and finite pieces  $F^\alpha$ ,

$$A^\alpha = c_\Gamma \left[ A^{\text{tree}, \alpha} V + i F^\alpha \right], \quad (2.10)$$

where  $\alpha = a, b$ , the prefactor is

$$c_\Gamma = \frac{1}{(4\pi)^{2-\epsilon}} \frac{\Gamma(1+\epsilon)\Gamma^2(1-\epsilon)}{\Gamma(1-2\epsilon)}, \quad (2.11)$$

and we work in dimensional regularization with  $D = 4 - 2\epsilon$ . The amplitudes presented here are ultraviolet-finite; all poles in  $\epsilon$  arise from virtual infrared (soft or collinear) singularities.

The divergent pieces are given by

$$V = -\frac{1}{\epsilon^2} \left( \frac{\mu^2}{-s_{12}} \right)^\epsilon - \frac{3}{2\epsilon} \left( \frac{\mu^2}{-s_{12}} \right)^\epsilon - \frac{7}{2}. \quad (2.12)$$

The finite piece of the triangle-parent contribution vanishes,

$$F^b = 0, \quad (2.13)$$

and the corresponding box-parent contribution is given by

$$\begin{aligned} F^a = & \left[ \frac{\langle 13 \rangle^2 [25]^2}{\langle 34 \rangle [56] t_{134} \langle 1|(5+6)|2 \rangle} - \frac{\langle 2|(5+6)|4 \rangle^2 \langle 6|(2+5)|1 \rangle^2}{[34] \langle 56 \rangle t_{134} \langle 2|(5+6)|1 \rangle^3} \right] \widetilde{\text{LS}}_{-1}^{2mh}(s_{12}, t_{134}; s_{34}, s_{56}) \\ & + \left[ \frac{1}{2} \frac{\langle 6|1|4 \rangle^2 t_{134}}{[34] \langle 56 \rangle \langle 2|(5+6)|1 \rangle} \frac{L_1\left(\frac{-s_{34}}{-t_{134}}\right)}{t_{134}^2} + 2 \frac{\langle 6|1|4 \rangle \langle 6|(2+5)|4 \rangle}{[34] \langle 56 \rangle \langle 2|(5+6)|1 \rangle} \frac{L_0\left(\frac{-t_{134}}{-s_{34}}\right)}{s_{34}} \right. \\ & - \frac{\langle 16 \rangle \langle 26 \rangle [14]^2 t_{134}}{[34] \langle 56 \rangle \langle 2|(5+6)|1 \rangle^2} \frac{L_0\left(\frac{-t_{134}}{-s_{34}}\right)}{s_{34}} - \frac{1}{2} \frac{\langle 26 \rangle [14] \langle 6|(2+5)|4 \rangle}{[34] \langle 56 \rangle \langle 2|(5+6)|1 \rangle^2} \ln\left(\frac{(-t_{134})(-s_{12})}{(-s_{34})^2}\right) \\ & \left. - \frac{3}{4} \frac{\langle 6|(2+5)|4 \rangle^2}{[34] \langle 56 \rangle t_{134} \langle 2|(5+6)|1 \rangle} \ln\left(\frac{(-t_{134})(-s_{12})}{(-s_{34})^2}\right) + L_{34/12} \ln\left(\frac{-s_{34}}{-s_{12}}\right) - \text{flip}_1 \right] \\ & + T I_3^{\text{3m}}(s_{12}, s_{34}, s_{56}) + \frac{1}{2} \frac{(t_{234}\delta_{12} + 2s_{34}s_{56})}{\langle 2|(5+6)|1 \rangle \Delta_3} \left( \frac{[45]^2}{[34] [56]} + \frac{\langle 36 \rangle^2}{\langle 34 \rangle \langle 56 \rangle} \right) \\ & + \frac{\langle 36 \rangle [45] (t_{134} - t_{234})}{\langle 2|(5+6)|1 \rangle \Delta_3} - \frac{1}{2} \frac{\langle 6|(2+5)|4 \rangle^2}{[34] \langle 56 \rangle t_{134} \langle 2|(5+6)|1 \rangle}, \quad (2.14) \end{aligned}$$

where ‘flip<sub>1</sub>’ is to be applied only to the terms inside the brackets ([ ]) in which it appears.



The coefficient of the logarithm reads

$$\begin{aligned}
L_{34/12} = & \frac{3}{2} \frac{\delta_{56} (t_{134} - t_{234}) \langle 3|(1+2)|4 \rangle \langle 6|(1+2)|5 \rangle}{\langle 2|(5+6)|1 \rangle \Delta_3^2} + \frac{3 \langle 36 \rangle [4|(1+2)(3+4)|5]}{2 \langle 2|(5+6)|1 \rangle \Delta_3} \\
& + \frac{1}{2} \frac{\langle 3|4|5 \rangle [4|(5+6)(1+2)|5]}{[56] \langle 2|(5+6)|1 \rangle \Delta_3} + \frac{[14] \langle 26 \rangle t_{134} (\langle 36 \rangle \delta_{12} - 2 \langle 3|45|6 \rangle)}{\langle 56 \rangle \langle 2|(5+6)|1 \rangle^2 \Delta_3} \\
& + \frac{1}{2} \frac{t_{134}}{\langle 2|(5+6)|1 \rangle \Delta_3} \left( \frac{\langle 34 \rangle [45]^2}{[56]} + \frac{[34] \langle 36 \rangle^2}{\langle 56 \rangle} - 2 \langle 36 \rangle [45] \right) \\
& + \left( \frac{\langle 3|(1+4)|5 \rangle}{[56]} - \frac{\langle 34 \rangle [14] \langle 26 \rangle}{\langle 2|(5+6)|1 \rangle} \right) \frac{[45] \delta_{12} - 2 [4|36|5]}{\langle 2|(5+6)|1 \rangle \Delta_3} \\
& + 4 \frac{\langle 3|4|5 \rangle \langle 6|(1+3)|4 \rangle + \langle 6|3|4 \rangle \langle 3|(2+4)|5 \rangle}{\langle 2|(5+6)|1 \rangle \Delta_3} \\
& + 2 \frac{\delta_{12}}{\langle 2|(5+6)|1 \rangle \Delta_3} \left( \frac{[45] \langle 3|(2+4)|5 \rangle}{[56]} - \frac{\langle 36 \rangle \langle 6|(1+3)|4 \rangle}{\langle 56 \rangle} \right), \tag{2.15}
\end{aligned}$$

and the three-mass triangle coefficient  $T$  is given by

$$\begin{aligned}
T = & \frac{3}{2} \frac{s_{12} \delta_{12} (t_{134} - t_{234}) \langle 6|(1+2)|5 \rangle \langle 3|(1+2)|4 \rangle}{\langle 2|(5+6)|1 \rangle \Delta_3^2} \\
& - \frac{1}{2} \frac{(3 s_{12} + 2 t_{134}) \langle 6|(1+2)|5 \rangle \langle 3|(1+2)|4 \rangle}{\langle 2|(5+6)|1 \rangle \Delta_3} \\
& + \frac{t_{134}}{\langle 2|(5+6)|1 \rangle^2 \Delta_3} \left[ [14] \langle 26 \rangle (\langle 3|6|5 \rangle \delta_{56} - \langle 3|4|5 \rangle \delta_{34}) \right. \\
& \quad \left. - [15] \langle 23 \rangle (\langle 6|5|4 \rangle \delta_{56} - \langle 6|3|4 \rangle \delta_{34}) \right] \\
& + \frac{\langle 36 \rangle [45] s_{12} t_{134}}{\langle 2|(5+6)|1 \rangle \Delta_3} - \frac{\langle 34 \rangle [56] \langle 6|(1+2)|4 \rangle^2}{\langle 2|(5+6)|1 \rangle \Delta_3} + 2 \frac{\langle 16 \rangle [24] (\langle 6|5|4 \rangle \delta_{56} - \langle 6|3|4 \rangle \delta_{34})}{[34] \langle 56 \rangle \Delta_3} \\
& + 2 \frac{\langle 6|(2+5)|4 \rangle}{\langle 2|(5+6)|1 \rangle \Delta_3} \left[ \frac{\langle 6|5|2 \rangle \langle 2|1|4 \rangle \delta_{56} - \langle 6|2|1 \rangle \langle 1|3|4 \rangle \delta_{34} + \langle 6|(2+5)|4 \rangle s_{12} \delta_{12}}{[34] \langle 56 \rangle} \right. \\
& \quad \left. + 2 \langle 3|(2+6)|5 \rangle s_{12} \right] \\
& - \frac{[14] \langle 26 \rangle \langle 3|(2+6)|5 \rangle}{\langle 2|(5+6)|1 \rangle^2} + 2 \frac{[15] \langle 23 \rangle \langle 6|(2+5)|4 \rangle}{\langle 2|(5+6)|1 \rangle^2} - \frac{[14] \langle 26 \rangle \langle 6|(2+5)|4 \rangle \delta_{12}}{[34] \langle 56 \rangle \langle 2|(5+6)|1 \rangle^2} \\
& + \frac{1}{2} \frac{1}{\langle 2|(5+6)|1 \rangle} \left[ 3 \frac{\langle 6|2|4 \rangle \langle 6|1|4 \rangle}{[34] \langle 56 \rangle} + \frac{\langle 3|2|5 \rangle \langle 3|1|5 \rangle}{\langle 34 \rangle [56]} + \frac{[14] \langle 16 \rangle [45]}{[34]} - \frac{[24] \langle 26 \rangle \langle 36 \rangle}{\langle 56 \rangle} \right. \\
& \quad \left. + \frac{\langle 23 \rangle [25] \langle 36 \rangle}{\langle 34 \rangle} - \frac{\langle 13 \rangle [15] [45]}{[56]} + 4 \langle 36 \rangle [45] \right] \\
& + \frac{1}{2} \frac{1}{\langle 1|(5+6)|2 \rangle} \left[ \frac{\langle 16 \rangle^2 [24]^2}{[34] \langle 56 \rangle} - \frac{\langle 13 \rangle^2 [25]^2}{\langle 34 \rangle [56]} \right] - \frac{1}{2} \frac{[14]^2 \langle 26 \rangle^2 (t_{134} \delta_{12} + 2 s_{34} s_{56})}{[34] \langle 56 \rangle \langle 2|(5+6)|1 \rangle^3}. \tag{2.16}
\end{aligned}$$

For the reader's convenience we recall the definitions of the functions appearing in eq. (2.14),

$$L_0(r) \equiv \frac{\ln(r)}{1-r}, \quad L_1(r) \equiv \frac{L_0(r) + 1}{1-r},$$

$$\begin{aligned} \text{LS}_{-1}(r_1, r_2) &\equiv \text{Li}_2(1 - r_1) + \text{Li}_2(1 - r_2) + \ln(r_1) \ln(r_2) - \frac{\pi^2}{6}, \\ \widetilde{\text{LS}}_{-1}^{2mh}(s, t, m_1^2, m_2^2) &\equiv -\text{Li}_2\left(1 - \frac{m_1^2}{t}\right) - \text{Li}_2\left(1 - \frac{m_2^2}{t}\right) \end{aligned} \quad (2.17)$$

$$- \frac{1}{2} \ln^2\left(\frac{-s}{-t}\right) + \frac{1}{2} \ln\left(\frac{-s}{-m_1^2}\right) \ln\left(\frac{-s}{-m_2^2}\right), \quad (2.18)$$

where the dilogarithm is

$$\text{Li}_2(x) = - \int_0^x dy \frac{\ln(1-y)}{y}. \quad (2.19)$$

The analytic structure of the three-mass-triangle integral  $I_3^{\text{3m}}$  is rather complicated in the general case (see Appendix A of ref. [20]). However, for the production of a vector boson pair  $V_1 V_2$  we have  $\Delta_3 = s_{12}(s_{12} - 2M_1^2 - 2M_2^2) + (M_1^2 - M_2^2)^2 > 0$ , i.e. we are in region (1b) of [20] and the integral is simply given by

$$\begin{aligned} I_3^{\text{3m}}(s_{12}, s_{34}, s_{56}) &= -\frac{1}{\sqrt{\Delta_3}} \text{Re} \left[ 2(\text{Li}_2(-\rho x) + \text{Li}_2(-\rho y)) + \ln(\rho x) \ln(\rho y) \right. \\ &\quad \left. + \ln\left(\frac{y}{x}\right) \ln\left(\frac{1+\rho y}{1+\rho x}\right) + \frac{\pi^2}{3} \right], \end{aligned} \quad (2.20)$$

where

$$x = \frac{s_{12}}{s_{56}}, \quad y = \frac{s_{34}}{s_{56}}, \quad \rho = \frac{2s_{56}}{\delta_{56} + \sqrt{\Delta_3}}. \quad (2.21)$$

The rational-function terms in eq. (2.14) have been rearranged some, so they no longer look exactly like the permutation of the addition of  $\delta p$  in eq. (2.5) to the rational-function terms of eq. (3.20) of [20].

## 2.4 Real (Bremsstrahlung) primitive amplitudes

A full next-to-leading order calculation of vector-boson pair production requires also the tree-level amplitudes with an additional gluon radiated from the quarks. The corresponding primitive amplitudes are easily calculated. For the case of a positive-helicity gluon with momentum  $k_7$  they are given by:

$$A_7^{\text{tree},a} = i \frac{\langle 13 \rangle}{\langle 17 \rangle s_{34} s_{56} t_{134}} \left[ \frac{\langle 13 \rangle [34] [25] \langle 6|(2+5)|7\rangle}{t_{256}} + \frac{\langle 6|(1+3)|4\rangle \langle 1|(2+7)|5\rangle}{\langle 72 \rangle} \right] \quad (2.22)$$

$$\begin{aligned} A_7^{\text{tree},b} &= \frac{i}{\langle 17 \rangle \langle 72 \rangle s_{34} s_{56} t_{127}} \left[ -\langle 36 \rangle [45] \langle 1|(5+6)(2+7)|1\rangle \right. \\ &\quad \left. + \langle 13 \rangle \langle 1|(2+7)|4\rangle \langle 6|(3+4)|5\rangle - \langle 16 \rangle \langle 1|(2+7)|5\rangle \langle 3|(5+6)|4\rangle \right]. \end{aligned} \quad (2.23)$$

The case of a negative-helicity gluon is given simply by applying the operation  $-\text{flip}_1$  to the positive-helicity case, where  $\text{flip}_1$  is defined in eq. (2.7). These amplitudes do have the appropriate limits when the gluon momentum  $k_7$  becomes soft, or becomes collinear with a quark momentum,  $k_1$  or  $k_2$ .

### 3 Dressing with electroweak couplings for $W^+W^-$ , $ZZ$ , $W^\pm Z$

This section is devoted to the construction of the (squared) amplitudes from the primitive amplitudes given in the previous section. We will discuss each process in turn. The formulas are given for the tree-level case with only four leptons in the final state. With some trivial modifications which will be discussed at the end of this section, the same formulas can be used for the one-loop (squared) amplitudes and the tree-level (squared) amplitudes with an additional gluon in the final state.

Concerning the labeling of the external particles: The incoming antiquark always gets label 1, while the incoming quark always gets label 2. The external gluon, if present, gets label 7. The final-state lepton labelings correspond to the minimal modifications of the  $WW$  case,

$$W^- + W^+ \rightarrow (\ell_3 \bar{\nu}_4) + (\bar{\ell}'_5 \nu'_6), \quad (3.1)$$

namely,

$$\begin{aligned} Z + Z &\rightarrow (\ell_3 \bar{\ell}_4) + (\bar{\ell}'_5 \ell'_6), \\ W^- + Z &\rightarrow (\ell_3 \bar{\nu}_4) + (\bar{\ell}'_5 \ell'_6), \end{aligned} \quad (3.2)$$

and the  $W^+Z$  case can be obtained by a CP transformation.

The results will be given in the unphysical configuration where all particles are outgoing. The momenta have to satisfy  $\sum_{i=1}^6 p_i = 0$ . In this configuration the label 1 corresponds to the outgoing quark; upon crossing to the physical region it becomes the label for the incoming antiquark. Recall that the helicity of the quarks will change sign under the crossing operation.

#### 3.1 $\bar{q}q \rightarrow W^-W^+ \rightarrow \ell \bar{\nu}_\ell \bar{\ell}' \nu_{\ell'}$

First consider up-quark annihilation into a  $W^+W^-$  pair. The leptons (anti-leptons) have to be left-handed (right-handed). If the (outgoing) up-quark is left-handed, the tree amplitude is

$$\begin{aligned} \mathcal{A}^{\text{tree}}(u_1^L, \bar{u}_2^R; \ell_3, \bar{\nu}_4; \bar{\ell}'_5, \nu'_6) &= \left( \frac{e^2}{\sin^2 \theta_W} \right)^2 \delta_{i_1 \bar{i}_2} \frac{s_{34}}{s_{34} - M_W^2 + i\Gamma_W M_W} \frac{s_{56}}{s_{56} - M_W^2 + i\Gamma_W M_W} \\ &\times \left[ A^{\text{tree},a}(1, 2, 3, 4, 5, 6) + C_{L,\{u\}} A^{\text{tree},b}(1, 2, 3, 4, 5, 6) \right], \end{aligned} \quad (3.3)$$

where

$$C_{L,\{u\}} = \pm 2Q \sin^2 \theta_W + \frac{s_{12}(1 \mp 2Q \sin^2 \theta_W)}{s_{12} - M_Z^2}, \quad (3.4)$$

$\theta_W$  is the weak mixing angle, and we take  $Q = 2/3$  and the upper sign in eq. (3.4) for the up quark. The color structure of the amplitude is simply given by  $\delta_{i_1 \bar{i}_2}$ , where  $i_1, \bar{i}_2$  are the color labels of the (anti-)quarks. Note that as  $s_{12} \rightarrow \infty$ ,  $C_{L,\{u\}} \rightarrow 1$ , and there is a high-energy cancellation between  $A^{\text{tree},a}$  and  $A^{\text{tree},b}$ :  $A^{\text{tree},a} \sim -A^{\text{tree},b}$  as  $s_{12} \rightarrow \infty$ . If the up-quark is

right-handed, the tree amplitude is

$$\begin{aligned} \mathcal{A}^{\text{tree}}(u_1^R, \bar{u}_2^L; \ell_3, \bar{\nu}_4; \bar{\ell}'_5, \nu'_6) &= \left( \frac{e^2}{\sin^2 \theta_W} \right)^2 \delta_{i_1 \bar{i}_2} \frac{s_{34}}{s_{34} - M_W^2 + i\Gamma_W M_W} \frac{s_{56}}{s_{56} - M_W^2 + i\Gamma_W M_W} \\ &\times C_{R,u} A^{\text{tree},b}(2, 1, 3, 4, 5, 6), \end{aligned} \quad (3.5)$$

where

$$C_{R,\{u\}} = \pm 2Q \sin^2 \theta_W \left[ 1 - \frac{s_{12}}{s_{12} - M_Z^2} \right]. \quad (3.6)$$

Since  $C_{R,\{u\}} \rightarrow 0$  as  $s_{12} \rightarrow \infty$ , the high-energy cancellation is simpler in this case. The finite width  $\Gamma_Z$  of the  $Z$  boson can safely be neglected in eqs. (3.4) and (3.6) because we have  $s_{12} > 4M_W^2$ . On the other hand, it is of course crucial to keep the  $i\Gamma_W M_W$  terms in the propagators of the  $W$  bosons.

The corresponding tree amplitudes for down-quark annihilation are

$$\begin{aligned} \mathcal{A}^{\text{tree}}(d_1^L, \bar{d}_2^R; \ell_3, \bar{\nu}_4; \bar{\ell}'_5, \nu'_6) &= \left( \frac{e^2}{\sin^2 \theta_W} \right)^2 \delta_{i_1 \bar{i}_2} \frac{s_{34}}{s_{34} - M_W^2 + i\Gamma_W M_W} \frac{s_{56}}{s_{56} - M_W^2 + i\Gamma_W M_W} \\ &\times \left[ A^{\text{tree},a}(1, 2, 6, 5, 4, 3) + C_{L,d} A^{\text{tree},b}(1, 2, 6, 5, 4, 3) \right] \end{aligned} \quad (3.7)$$

and

$$\begin{aligned} \mathcal{A}^{\text{tree}}(d_1^R, \bar{d}_2^L; \ell_3, \bar{\nu}_4; \bar{\ell}'_5, \nu'_6) &= \left( \frac{e^2}{\sin^2 \theta_W} \right)^2 \delta_{i_1 \bar{i}_2} \frac{s_{34}}{s_{34} - M_W^2 + i\Gamma_W M_W} \frac{s_{56}}{s_{56} - M_W^2 + i\Gamma_W M_W} \\ &\times C_{R,d} A^{\text{tree},b}(2, 1, 6, 5, 4, 3), \end{aligned} \quad (3.8)$$

where we take  $Q = -1/3$  and the lower sign in eqs. (3.4) and (3.6) for the down quark. Note that because of Cabibbo-Kobayashi-Maskawa mixing and the large mass of the top quark, we have not done the  $t$ -channel exchange of the top quark correctly. Fortunately this error is proportional to the tiny quantity  $|V_{td}|^2$  (or for  $d\bar{s}$  annihilation, to  $V_{td}V_{ts}^*$  times a suppression factor for the strange sea quark distribution in the proton).

We can now construct the differential cross-section in the narrow-width approximation. We normalize the squared amplitudes  $\mathcal{M}^{\text{tree}}$  such that the integral over center-of-mass angles for the lepton-pair decay products of both vector bosons only has to be multiplied by the two-body phase-space factor, in order to obtain the total partonic vector-boson pair production cross-section multiplied by the leptonic branching ratios,

$$d\sigma_2(q\bar{q} \rightarrow V_1 V_2) \times B_\ell(V_1) B_{\ell'}(V_2) = d\Phi_2 \int d^2\Omega_1 \int d^2\Omega_2 \mathcal{M}^{\text{tree}}. \quad (3.9)$$

The two-body phase-space factor is given by

$$d\Phi_2 = \frac{\beta}{16\pi} d\cos\theta_{CM}, \quad (3.10)$$

where

$$\beta = \frac{\sqrt{(s_{12} - (M_1 + M_2)^2)(s_{12} - (M_1 - M_2)^2)}}{s_{12}} \quad (3.11)$$

and

$$\int d^2\Omega_1 = \int_0^\pi d\theta_1 \sin\theta_1 \int_0^{2\pi} d\phi_1. \quad (3.12)$$

Here  $(\theta_1, \phi_1)$  are the angles of one of the decay leptons, measured in that vector boson  $V_1$ 's center-of-mass frame. For equal masses  $M_1 = M_2$ ,  $\beta$  is the velocity of  $V_1$  and  $V_2$  in the  $q\bar{q}$  center-of-mass frame.

We obtain for the squared Born amplitude for unpolarized  $\bar{u}u \rightarrow WW$ ,

$$\begin{aligned} \mathcal{M}^{\text{tree}}(u_1, \bar{u}_2; \ell_3, \bar{\nu}_4; \bar{\ell}'_5, \nu'_6) &= B_\ell^2(W) \left( \frac{e^2}{\sin^2\theta_W} \right)^2 \left( \frac{3}{4\pi} \right)^2 \frac{M_W^4}{8 s_{12} N_c} \\ &\times \left\{ \left| A^{\text{tree},a}(1, 2, 3, 4, 5, 6) + C_{L,u} A^{\text{tree},b}(1, 2, 3, 4, 5, 6) \right|^2 + \left| C_{R,u} A^{\text{tree},b}(2, 1, 3, 4, 5, 6) \right|^2 \right\}, \end{aligned} \quad (3.13)$$

while for unpolarized  $\bar{d}d \rightarrow WW$ , we obtain

$$\begin{aligned} \mathcal{M}^{\text{tree}}(d_1, \bar{d}_2; \ell_3, \bar{\nu}_4; \bar{\ell}'_5, \nu'_6) &= B_\ell^2(W) \left( \frac{e^2}{\sin^2\theta_W} \right)^2 \left( \frac{3}{4\pi} \right)^2 \frac{M_W^4}{8 s_{12} N_c} \\ &\times \left\{ \left| A^{\text{tree},a}(1, 2, 6, 5, 4, 3) + C_{L,d} A^{\text{tree},b}(1, 2, 6, 5, 4, 3) \right|^2 + \left| C_{R,d} A^{\text{tree},b}(2, 1, 6, 5, 4, 3) \right|^2 \right\}, \end{aligned} \quad (3.14)$$

with  $N_c = 3$  for QCD. The corresponding expressions for longitudinally-polarized scattering can be obtained simply by dropping the ‘‘unwanted’’ terms in eqs. (3.13) and (3.14), and adjusting the normalization appropriately.

### 3.2 $\bar{q}q \rightarrow ZZ \rightarrow \ell\bar{\ell}\ell'\ell'$

In the  $\bar{q}q \rightarrow ZZ$  process, only the symmetric combination appears,

$$A^{\text{tree},s} = A^{\text{tree},a}(1, 2, 3, 4, 5, 6) + A^{\text{tree},a}(1, 2, 6, 5, 4, 3). \quad (3.15)$$

(This sum includes the ‘exchange’ graphs just as in  $A_6^{\text{sl}}$ ; hence the simpler form found for this quantity in [22] could be used here, once diagram (b) is removed and the appropriate permutation is applied.) In the  $ZZ$  case, there are more non-vanishing helicity configurations. We refrain from writing down all the individual helicity amplitudes in this case, and just present the differential cross-section formulas for the various helicity configurations, normalized as discussed above:

$$\begin{aligned} \mathcal{M}^{\text{tree}}(q_1^L, \bar{q}_2^R; \ell_3^-, \bar{\ell}_4^+, \bar{\ell}_5^+, \ell_6^-) &= p_{ZZ} v_{L,q}^4 v_{L,e}^4 |A^{\text{tree},s}(1, 2, 3, 4, 5, 6)|^2, \\ \mathcal{M}^{\text{tree}}(q_1^L, \bar{q}_2^R; \ell_3^+, \bar{\ell}_4^-, \bar{\ell}_5^+, \ell_6^-) &= p_{ZZ} v_{L,q}^4 v_{L,e}^2 v_{R,e}^2 |A^{\text{tree},s}(1, 2, 4, 3, 5, 6)|^2, \\ \mathcal{M}^{\text{tree}}(q_1^L, \bar{q}_2^R; \ell_3^-, \bar{\ell}_4^+, \bar{\ell}_5^-, \ell_6^+) &= p_{ZZ} v_{L,q}^4 v_{L,e}^2 v_{R,e}^2 |A^{\text{tree},s}(1, 2, 3, 4, 6, 5)|^2, \\ \mathcal{M}^{\text{tree}}(q_1^L, \bar{q}_2^R; \ell_3^+, \bar{\ell}_4^-, \bar{\ell}_5^-, \ell_6^+) &= p_{ZZ} v_{L,q}^4 v_{R,e}^4 |A^{\text{tree},s}(1, 2, 4, 3, 6, 5)|^2, \end{aligned} \quad (3.16)$$

where we defined

$$p_{ZZ} = B_\ell^2(Z) e^4 \left( \frac{3}{4\pi} \right)^2 \frac{M_Z^4}{4 s_{12} N_c (v_{L,e}^2 + v_{R,e}^2)^2}. \quad (3.17)$$

The formulas for  $\mathcal{M}^{\text{tree}}(q_1^R, \bar{q}_2^L; \dots)$  can be obtained by replacing  $v_{L,q}^4$  by  $v_{R,q}^4$  and interchanging the labels 1 and 2 in eq. (3.16). The unpolarized cross-section, normalized as in eq. (3.9), is given by the sum over all these  $\mathcal{M}^{\text{tree}}$ 's. In the above, the left- and right-handed couplings to the  $Z$  are

$$\begin{aligned} v_{L,e} &= \frac{-1 + 2 \sin^2 \theta_W}{\sin 2\theta_W}, & v_{R,e} &= \frac{2 \sin^2 \theta_W}{\sin 2\theta_W}, \\ v_{L,q} &= \frac{\pm 1 - 2Q \sin^2 \theta_W}{\sin 2\theta_W}, & v_{R,q} &= -\frac{2Q \sin^2 \theta_W}{\sin 2\theta_W}, \end{aligned} \quad (3.18)$$

where  $Q$  is the charge of quark  $q$  in units of  $e$ , and the two signs in  $v_{L,q}$  correspond to up (+) and down (-) type quarks.

### 3.3 $\bar{u}d \rightarrow W^- Z \rightarrow \ell \bar{\nu}_\ell \bar{\ell}' \ell'$

Finally, for  $WZ$  production the down-quark and the lepton  $\ell$  have to be left-handed. The lepton  $\ell'$  which couples to the  $Z$  can have either polarization. If it is left-handed, the cross-section is proportional to  $v_{L,e}^2$  while for a right-handed  $\ell'$  it is proportional to  $v_{R,e}^2$ . For the unpolarized cross-section we have

$$\begin{aligned} \mathcal{M}^{\text{tree}}(u_1, \bar{d}_2; \ell_3, \bar{\nu}_3; \bar{\ell}'_4, \ell'_5) &= B_\ell(W) B_{\ell'}(Z) |V_{ud}|^2 \left( \frac{e^2}{\sin \theta_W} \right)^2 \left( \frac{3}{4\pi} \right)^2 \frac{M_W^2 M_Z^2}{4 s_{12} N_c (v_{L,e}^2 + v_{R,e}^2)} \\ &\times \left\{ v_{L,e}^2 \left| v_{L,d} A^{\text{tree},a}(1, 2, 3, 4, 5, 6) + v_{L,u} A^{\text{tree},a}(1, 2, 6, 5, 4, 3) \right. \right. \\ &\quad \left. \left. - \cot \theta_W \frac{s_{12}}{s_{12} - M_W^2} A^{\text{tree},b}(1, 2, 3, 4, 5, 6) \right|^2 \right. \\ &\quad \left. + v_{R,e}^2 \left| v_{L,d} A^{\text{tree},a}(1, 2, 3, 4, 6, 5) + v_{L,u} A^{\text{tree},a}(1, 2, 5, 6, 4, 3) \right. \right. \\ &\quad \left. \left. - \cot \theta_W \frac{s_{12}}{s_{12} - M_W^2} A^{\text{tree},b}(1, 2, 3, 4, 6, 5) \right|^2 \right\}. \end{aligned} \quad (3.19)$$

The results for the polarized cross-section can easily be extracted from eq. (3.19).

### 3.4 Loop and Bremsstrahlung amplitudes

The QCD loop corrections to all the amplitudes under consideration are given by a simple substitution of loop primitive amplitudes for tree primitive amplitudes,

$$\mathcal{A}^{\text{loop}} = g^2 \frac{N_c^2 - 1}{N_c} \mathcal{A}^{\text{tree}} \Big|_{A^{\text{tree},\alpha} \rightarrow A^\alpha}, \quad \alpha = a, b, \quad (3.20)$$

where  $g$  is the strong coupling, and  $N_c = 3$  for QCD. Thus, the next-to-leading order virtual corrections to the above cross-sections are obtained by replacing  $(A^{\text{tree},\alpha})^* A^{\text{tree},\alpha}$  in eqs. (3.13), (3.14), (3.16) and (3.19) by  $2 \text{Re}[(A^{\text{tree},\alpha})^* A^\alpha]$  and multiplying by  $g^2 \frac{N_c^2 - 1}{N_c} = 8\pi\alpha_s C_F$ .

The leading high-energy behavior of the loop amplitude cancels in the same way as the tree amplitude. First note that none of the terms in  $F^a$  contains the factor  $\frac{1}{s_{34} s_{56}}$ , which is

present in  $A^{\text{tree},a}$ . Thus the high-energy limit is governed completely by the  $V$  pieces. This ensures that the tree-level cancellation continues to take place at the loop level.

We remark that any non-Standard Model modifications of the three-boson vertex would only affect the second ( $b$ ) class of diagrams. The virtual QCD corrections can therefore be obtained in this case simply by multiplying the modified tree amplitude by the factor  $V$  given in eq. (2.12).

The squared amplitudes for the processes with an additional external gluon can be obtained by a similar change. In this case one has to replace  $A^{\text{tree},\alpha}$  and  $(A^{\text{tree},\alpha})^*$  by  $A_7^{\text{tree},\alpha}$  and  $(A_7^{\text{tree},\alpha})^*$  respectively and multiply again by  $g^2 \frac{N_c^2 - 1}{N_c}$ . Furthermore,  $s_{12}$  has to be replaced by  $t_{127}$  in the expressions for  $C_{L,\{d\}}$  and  $C_{R,\{d\}}$ , eqs. (3.4) and (3.6), as well as in eq. (3.19). The normalization is the same as long as the two-body phase-space factor  $d\Phi_2$  in eq. (3.10) is replaced by the three-body phase-space factor  $d\Phi_3$ . Because eqns. (2.22) and (2.23) for  $A_7^{\text{tree},\alpha}$  are crossing-symmetric, these substitutions are equally valid for processes where the gluon is in the final state,  $q\bar{q} \rightarrow V_1 V_2 g$ , or in the initial state,  $gq \rightarrow V_1 V_2 q$  and  $g\bar{q} \rightarrow V_1 V_2 \bar{q}$ , provided that the factor coming from the spin-color average is changed accordingly; all three processes contribute at next-to-leading order.

## 4 Real photons in the final state

The cases with a single real photon,  $W\gamma$  and  $Z\gamma$ , can be handled as well, but the required primitive amplitudes are different. The one-loop primitive amplitude needed for the  $Z\gamma$  case can be extracted from the existing subleading-in-color primitive amplitude for  $e^+e^- \rightarrow q\bar{q}g$ , as given in appendix IV of [22]. This helicity amplitude was first calculated in [21]. In the  $W\gamma$  case, just as for the  $W^+W^-$  and  $W^-Z$  cases above, the  $e^+e^- \rightarrow q\bar{q}g$  amplitude has to be split further into two ‘fully primitive’ pieces (which in this case are not related by a symmetry).

### 4.1 Virtual primitive amplitudes for $q\bar{q} \rightarrow V_1\gamma$

For  $q\bar{q} \rightarrow V_1\gamma$  there is no ‘exchange’ symmetry to relate the contributions with the reversed ordering of  $V_1$  and the photon on the quark line. On the other hand, under an on-shell gauge transformation for the photon (i.e., substitution of its polarization vector by its momentum), the diagrams where the photon is radiated from the quark line mix with those where it is radiated from the  $V_1 = W$  line. Let the photon be leg 5, the  $q\bar{q}$  pair be  $\{1, 2\}$ , and the leptonic decay products of  $V_1$  be  $\{3, 4\}$ . Then we again define two primitive amplitudes,

$$A_\gamma^\alpha(1^-, 2^+, 3^-, 4^+, 5^+), \quad \alpha = a, b, \quad (4.1)$$

where  $A_\gamma^a$  ( $A_\gamma^b$ ) includes all ordered diagrams where the photon is on the leg 2 (leg 1) side of the diagram. The negative-helicity photon cases are obtained by another ‘flip’ permutation,

$$\begin{aligned} A_\gamma^a(1^-, 2^+, 3^-, 4^+, 5^-) &= \text{flip}_2 \left[ A_\gamma^b(1^-, 2^+, 3^-, 4^+, 5^+) \right], \\ A_\gamma^b(1^-, 2^+, 3^-, 4^+, 5^-) &= \text{flip}_2 \left[ A_\gamma^a(1^-, 2^+, 3^-, 4^+, 5^+) \right], \end{aligned} \quad (4.2)$$

where

$$\text{flip}_2 : \quad 1 \leftrightarrow 2, \quad 3 \leftrightarrow 4, \quad \langle ab \rangle \leftrightarrow [ab]. \quad (4.3)$$

Therefore we present only the positive-helicity photon case below.

The tree amplitudes are given by

$$A_\gamma^{\text{tree},a} = -i \frac{\langle 13 \rangle^2 [15]}{\langle 34 \rangle \langle 25 \rangle (s_{12} - s_{34})}, \quad (4.4)$$

$$A_\gamma^{\text{tree},b} = -i \frac{\langle 13 \rangle^2 [25]}{\langle 34 \rangle \langle 15 \rangle (s_{12} - s_{34})}, \quad (4.5)$$

where  $s_{34}$  should be set equal to  $M_{V_1}^2$  in accordance with the narrow-width approximation.

For the one-loop photon amplitudes we use the same decomposition (2.10) into a divergent part  $V$ , and finite parts  $F$  which are given by

$$F_\gamma^a = \frac{\langle 13 \rangle^2}{\langle 15 \rangle \langle 34 \rangle \langle 25 \rangle} \text{Ls}_{-1} \left( \frac{-s_{25}}{-s_{34}}, \frac{-s_{12}}{-s_{34}} \right) + \frac{1}{2} \frac{\langle 12 \rangle \langle 35 \rangle [45] [25]}{\langle 25 \rangle} \frac{\text{L}_1 \left( \frac{-s_{34}}{-s_{12}} \right)}{s_{12}^2} - \frac{3}{2} \frac{\langle 13 \rangle [45]}{\langle 25 \rangle} \frac{\text{L}_0 \left( \frac{-s_{34}}{-s_{12}} \right)}{s_{12}} - \frac{1}{2} \frac{[24] [45]}{[12] [34] \langle 25 \rangle}, \quad (4.6)$$

$$F_\gamma^b = \frac{\langle 12 \rangle^2 \langle 35 \rangle^2}{\langle 34 \rangle \langle 15 \rangle \langle 25 \rangle^3} \text{Ls}_{-1} \left( \frac{-s_{12}}{-s_{34}}, \frac{-s_{15}}{-s_{34}} \right) - \frac{1}{2} \frac{\langle 23 \rangle^2 [25]^2 \langle 15 \rangle}{\langle 34 \rangle \langle 25 \rangle} \frac{\text{L}_1 \left( \frac{-s_{34}}{-s_{15}} \right)}{s_{15}^2} + \frac{\langle 23 \rangle [25] (\langle 12 \rangle \langle 35 \rangle + \langle 13 \rangle \langle 25 \rangle)}{\langle 34 \rangle \langle 25 \rangle^2} \frac{\text{L}_0 \left( \frac{-s_{34}}{-s_{15}} \right)}{s_{15}} - \frac{1}{2} \frac{\langle 12 \rangle^2 \langle 35 \rangle^2 [25]}{\langle 34 \rangle \langle 15 \rangle \langle 25 \rangle^2} \left[ s_{15} \frac{\text{L}_1 \left( \frac{-s_{34}}{-s_{12}} \right)}{s_{12}^2} + 3 \frac{\text{L}_0 \left( \frac{-s_{34}}{-s_{12}} \right)}{s_{12}} \right] - \frac{1}{2} \frac{\langle 23 \rangle [25] \langle 35 \rangle}{[12] \langle 34 \rangle \langle 25 \rangle^2} - \frac{1}{2} \frac{[14] [25] [45]}{[12] [34] [15] \langle 25 \rangle}. \quad (4.7)$$

The integral functions appearing in the above equations are defined in eqs. (2.17).

These amplitudes can be extracted from the collinear limit of the virtual-photon case,  $q\bar{q} \rightarrow W\gamma^*$ , when the momenta of the virtual photon's decay leptons 5 and 6 become parallel. The relevant primitive-amplitude combination is  $A^a + \frac{s_{12}}{s_{12}-s_{34}} A^b$  (see eq. (3.19)). In the collinear limit, with  $k_P \equiv k_5 + k_6$ , it becomes

$$A^a + \frac{s_{12}}{s_{12} - s_{34}} A^b \xrightarrow{5\parallel 6} \frac{z}{[56]} A_\gamma^a(1^-, 2^+, 3^-, 4^+, P^+) + \frac{1-z}{\langle 56 \rangle} A_\gamma^a(1^-, 2^+, 3^-, 4^+, P^-). \quad (4.8)$$

Using the ‘flip’ relation, we can read off the two independent photon amplitudes.

The sum of  $A_\gamma^a$  and  $A_\gamma^b$  (which is all that is required for the case  $q\bar{q} \rightarrow Z\gamma$ ) reproduces, after relabelings, the existing subleading-in-color primitive amplitude for  $e^+e^- \rightarrow q\bar{q}g$ , as given in appendix IV of [22].



## 4.2 Real (Bremsstrahlung) primitive amplitudes

The tree-level amplitudes with an additional gluon radiated from the quarks,  $q\bar{q} \rightarrow V_1\gamma g$ , can similarly be obtained from the collinear limit of the  $q\bar{q} \rightarrow V_1\gamma^*g$  case, which is described by  $A_7^{\text{tree},a} + \frac{t_{127}}{t_{127}-s_{34}}A_7^{\text{tree},b}$ . Let the gluon label be 6. In analogy to the definitions for the virtual case,  $A_{6,\gamma}^{\text{tree},a}$  ( $A_{6,\gamma}^{\text{tree},b}$ ) includes all ordered diagrams where the photon is on the leg 2 (leg 1) side of the diagram. The results are

$$A_{6,\gamma}^{\text{tree},a}(1^-, 2^+, 3^-, 4^+, 5^+, 6^+) = i \frac{\langle 13 \rangle^2 \langle 2|(3+4)|5 \rangle}{\langle 34 \rangle \langle 25 \rangle \langle 16 \rangle \langle 62 \rangle (t_{126} - s_{34})}, \quad (4.9)$$

$$A_{6,\gamma}^{\text{tree},a}(1^-, 2^+, 3^-, 4^+, 5^-, 6^+) = -i \left[ \frac{\langle 13 \rangle [62] \langle 5|(1+3)|4 \rangle}{s_{34} [25] \langle 62 \rangle t_{134}} + \frac{\langle 1|(2+6)|4 \rangle (\langle 34 \rangle \langle 15 \rangle [42] + \langle 35 \rangle \langle 16 \rangle [62])}{s_{34} [25] \langle 16 \rangle \langle 62 \rangle (t_{126} - s_{34})} \right], \quad (4.10)$$

$$A_{6,\gamma}^{\text{tree},b}(1^-, 2^+, 3^-, 4^+, 5^+, 6^+) = -i \frac{\langle 13 \rangle^2 \langle 1|(3+4)|5 \rangle}{\langle 34 \rangle \langle 15 \rangle \langle 16 \rangle \langle 62 \rangle (t_{126} - s_{34})}, \quad (4.11)$$

$$A_{6,\gamma}^{\text{tree},b}(1^-, 2^+, 3^-, 4^+, 5^-, 6^+) = i \left[ \frac{\langle 15 \rangle [24] \langle 3|(1+5)|6 \rangle}{s_{34} [15] \langle 16 \rangle t_{234}} + \frac{\langle 1|(2+6)|4 \rangle (\langle 5|(2+6)4|3 \rangle + \langle 53 \rangle s_{26})}{s_{34} [15] \langle 16 \rangle \langle 62 \rangle (t_{126} - s_{34})} \right]. \quad (4.12)$$

The cases where the gluon has negative helicity are obtained by applying  $+\text{flip}_2$  to the above amplitudes (which simultaneously reverses the photon helicity).

## 4.3 Dressing with electroweak couplings

As in the case of two massive vector bosons, we present the fully dressed amplitudes and differential cross-sections at tree level. The substitutions required to obtain the one-loop (squared) amplitudes and tree-level (squared) amplitudes with an additional gluon are exactly the same as those described in section 3.4.

### 4.3.1 $\bar{u}d \rightarrow W^- \gamma \rightarrow \ell \bar{\nu}_\ell \gamma$

For the process  $\bar{u}d \rightarrow W^- \gamma$ , the lepton (anti-lepton) has to be left-handed (right-handed), and the (outgoing) up-quark must also be left-handed. The tree amplitude is

$$A^{\text{tree}}(u_1, \bar{d}_2; \ell_3, \bar{\nu}_4; \gamma_5^\pm) = \sqrt{2} \left( \frac{e^3}{\sin^2 \theta_W} \right) V_{ud} \delta_{i_1}^{\bar{i}_2} \frac{s_{34}}{s_{34} - M_W^2 + i\Gamma_W M_W} \times \left[ Q_2 A_\gamma^{\text{tree},a}(1, 2, 3, 4, 5^\pm) + Q_1 A_\gamma^{\text{tree},b}(1, 2, 3, 4, 5^\pm) \right], \quad (4.13)$$

where  $Q_1 = 2/3$  ( $Q_2 = -1/3$ ) is the up (down) quark charge. From this amplitude we obtain the spin-summed squared amplitude,

$$\mathcal{M}^{\text{tree}}(u_1, \bar{d}_2; \ell_3, \bar{\nu}_4; \gamma_5) = B_\ell(W) |V_{ud}|^2 \left( \frac{e^2}{\sin \theta_W} \right)^2 \left( \frac{3}{4\pi} \right) \frac{M_W^2}{4 s_{12} N_c} \sum_{\lambda=\pm} \left| Q_2 A_\gamma^a(1, 2, 3, 4, 5^\lambda) + Q_1 A_\gamma^b(1, 2, 3, 4, 5^\lambda) \right|^2. \quad (4.14)$$

The normalization of this cross-section is the same as in the  $W^+W^-$  case, eq. (3.9), except that the integral  $\int d^2\Omega_2$  and the factor  $B_{\ell}(V_2)$  should be omitted.

### 4.3.2 $\bar{q}q \rightarrow Z\gamma \rightarrow \ell\bar{\ell}\gamma$

In the  $\bar{q}q \rightarrow Z\gamma$  process, only the symmetric combination appears,

$$A_{\gamma}^{\text{tree},s}(1, 2, 3, 4, 5^{\pm}) = A_{\gamma}^{\text{tree},a}(1, 2, 3, 4, 5^{\pm}) + A_{\gamma}^{\text{tree},b}(1, 2, 3, 4, 5^{\pm}). \quad (4.15)$$

We again refrain from writing down all the individual helicity amplitudes here, and just present the differential cross-section formulas for the various helicity configurations, normalized as discussed above:

$$\begin{aligned} \mathcal{M}_{\gamma}^{\text{tree}}(q_1^L, \bar{q}_2^R; \ell_3^-, \bar{\ell}_4^+; \gamma_5^{\pm}) &= p_{Z\gamma} Q^2 v_{L,q}^2 v_{L,e}^2 |A_{\gamma}^{\text{tree},s}(1, 2, 3, 4, 5^{\pm})|^2, \\ \mathcal{M}_{\gamma}^{\text{tree}}(q_1^L, \bar{q}_2^R; \ell_3^+, \bar{\ell}_4^-; \gamma_5^{\pm}) &= p_{Z\gamma} Q^2 v_{L,q}^2 v_{R,e}^2 |A_{\gamma}^{\text{tree},s}(1, 2, 4, 3, 5^{\pm})|^2, \end{aligned} \quad (4.16)$$

where we defined

$$p_{Z\gamma} = B_{\ell}(Z) e^4 \left( \frac{3}{4\pi} \right) \frac{M_Z^2}{2 s_{12} N_c (v_{L,e}^2 + v_{R,e}^2)}. \quad (4.17)$$

The formulas for  $\mathcal{M}^{\text{tree}}(q_1^R, \bar{q}_2^L; \dots)$  can be obtained by replacing  $v_{L,q}^2$  by  $v_{R,q}^2$  and interchanging the labels 1 and 2 in eq. (4.16).

## 5 Concluding remarks

We have presented all helicity amplitudes which are needed for a complete computation of the next-to-leading order QCD corrections to the production of a  $Z Z$ ,  $W^+W^-$ ,  $W^{\pm}Z$ ,  $W^{\pm}\gamma$  or  $Z\gamma$  pair at hadron colliders, where the spin correlations are fully taken into account. The subsequent decay of each massive vector boson into a lepton pair is included in the narrow-width approximation.

The above cross-sections have been ‘‘integrated’’ over the lepton decay angles, after which they reproduce the previously published analytic formulae for the virtual corrections of refs. [8, 10, 12, 13] to 30 digits accuracy. Such a high accuracy can be achieved because the true integration can be replaced by  $6 \times 6 = 36$  numerical evaluations, in which each lepton is emitted along three orthogonal axes (both positive and negative directions) in the corresponding vector-boson center-of-mass frame. As a check of the bremsstrahlung amplitudes we compared in the same way the real contribution in the  $W^+W^-$  case to ref. [12] and found full agreement.

Of course the new information provided by the above cross-sections is not the total cross-section, but rather the correlations between the lepton decay angles (or lab-frame momenta). There are at least two different ways to access this information at next-to-leading order:

(1) Construct a general purpose Monte Carlo program directly in terms of the lepton momenta.

(2) Compute the elements of the density matrix  $D_{i_1, i_2; j_1, j_2}(s, \dots)$ . These are the amplitude interferences for the production of a vector boson  $V_1$  with helicity  $i_1$  or  $j_1 = -1, 0, +1$  along

its direction of motion (in the  $q\bar{q} \rightarrow V_1 V_2$  frame, for example), and  $V_2$  with helicity  $i_2$  or  $j_2$ . The complete  $\mathcal{O}(\alpha_s)$  density matrix for polarized vector boson production can easily be computed using the results presented in this paper. One simply has to carry out the integration over the angles of the lepton pair, except that one now weights the numerical evaluations with an additional projection operator,  $\exp[i(-i_1 + j_1)\phi_1 + i(-i_2 + j_2)\phi_2]$ , where  $\phi_{1,2}$  is the azimuthal angle of a decay lepton with respect to the direction of motion of  $V_{1,2}$ . One can then fold the computed production density matrix with the decay density matrices. A possible advantage of the second approach is that it is straightforward to include the additional QCD corrections that are present for hadronically decaying vector bosons, such as those computed in [29] for the  $W$  boson.

For this latter application, to processes such as  $q\bar{q} \rightarrow W^+ W^- \rightarrow q' \bar{q}'' \ell \bar{\nu}_\ell$  (and neglecting interferences with non-resonant processes), the required amplitudes may be obtained from those described in this paper by appropriate modifications of the coupling constant factors. (At  $\mathcal{O}(\alpha_s)$ , gluon exchange between the initial and final quark lines gives a vanishing correction.) Because quark final states are phenomenologically somewhat less relevant, these amplitudes have not been explicitly presented here. Similarly, one can easily extend these results to cover the cases where the lepton pair coming from an on-shell  $Z$  boson is replaced by a Drell-Yan pair of arbitrary invariant mass from an intermediate virtual photon plus  $Z$ .

The amplitudes presented here can easily be implemented in a Monte Carlo program. This would extend previous results [18] in that the spin correlations of the virtual part would also be fully included. Furthermore, the simplicity of the amplitudes should aid in the next-to-leading-order study of the effects of non-standard triple-gauge-boson couplings.

## Acknowledgments

We would like to thank S. Frixione for useful discussions and D.A. Kosower for use of his tex-to-maple converter. A.S. would like to thank the Theory Group of ETH Zürich, where part of this work has been done, for its hospitality. Z.K. is grateful to the CERN Theory Group for its hospitality.

## References

- [1] F. Abe et al. (CDF collaboration) *Phys. Rev. Lett.* **75** (1995) 1034 [hep-ex/9505007];  
F. Abe et al. (CDF collaboration) *Phys. Rev. Lett.* **78** (1997) 4536.
- [2] S. Abachi et al. (D0 collaboration) *Phys. Rev. Lett.* **78** (1997) 3634 [hep-ex/9612002];  
B. Abbott et al. (D0 collaboration) *Phys. Rev. Lett.* **79** (1997) 1441 [hep-ex/9705010].
- [3] L. Nodulman (for CDF and D0 collaborations), in *ICHEP '96: Proceedings*, eds. Z. Ajduk and A.K. Wroblewski (World Scientific, 1997);  
G. Landsberg (for D0 and CDF collaborations), FERMILAB-CONF-97-340-E, to appear in proceedings of 16th Intl. Workshop on Weak Interactions and Neutrinos (WIN

- 97), June 1997;  
T. Yasuda (for CDF and D0 collaborations), preprint hep-ex/9706015, to appear in proceedings of Hadron Collider Physics XII, June 1997.
- [4] See e.g., K. Hagiwara, J. Woodside and D. Zeppenfeld, *Phys. Rev.* **D41** (1990) 2113, and references therein.
- [5] E. Eichten, I. Hinchliffe, K. Lane and C. Quigg, *Rev. Mod. Phys.* **56** (1984) 579.
- [6] R.W. Brown and K.O. Mikaelian, *Phys. Rev.* **D19** (1979) 922.  
R.W. Brown, K.O. Mikaelian and D. Sahdev, *Phys. Rev.* **D20** (1979) 1164.  
K.O. Mikaelian, M.A. Samuel and D. Sahdev, *Phys. Rev. Lett.* **43** (1979) 746.
- [7] J. Ohnemus and J.F. Owens, *Phys. Rev.* **D43** (1991) 3626.
- [8] B. Mele, P. Nason and G. Ridolfi, *Nucl. Phys.* **B357** (1991) 409.
- [9] J. Ohnemus, *Phys. Rev.* **D44** (1991) 3477.
- [10] S. Frixione, P. Nason and G. Ridolfi, *Nucl. Phys.* **B383** (1992) 3.
- [11] J. Ohnemus, *Phys. Rev.* **D44** (1991) 1403.
- [12] S. Frixione, *Nucl. Phys.* **B410** (1993) 280.
- [13] J. Smith, D. Thomas and W.L. van Neerven, *Zeit. Phys.* **C44** (1989) 267.
- [14] J. Ohnemus, *Phys. Rev.* **D47** (1992) 940.
- [15] E.W.N. Glover, J. Ohnemus and S.D. Willenbrock, *Phys. Rev.* **D37** (1988) 3193;  
V. Barger, G. Bhattacharya, T. Han and B.A. Kniehl, *Phys. Rev.* **D43** (1991) 779.
- [16] M. Dittmar and H. Dreiner, *Phys. Rev.* **D55** (1997) 167 [hep-ph/9608317]; hep-ph/9703401, in *Tegernsee 1996, The Higgs Puzzle*.
- [17] J.F. Gunion and Z. Kunszt, *Phys. Rev.* **D33** (1986) 665.
- [18] J. Ohnemus, *Phys. Rev.* **D50** (1994) 1931 [hep-ph/9403331];  
U. Baur, T. Han and J. Ohnemus, preprint hep-ph/9710416.
- [19] P. De Causmaecker, R. Gastmans, W. Troost and T.T. Wu, *Phys. Lett.* **105B** (1981) 215, *Nucl. Phys.* **B206** (1982) 53;  
J.F. Gunion and Z. Kunszt, *Phys. Lett.* **161B** (1985) 333;  
R. Kleiss and W.J. Stirling, *Nucl. Phys.* **B262** (1985) 235;  
R. Gastmans and T.T. Wu, *The Ubiquitous Photon: Helicity Method for QED and QCD* (Clarendon Press, 1990);  
Z. Xu, D.-H. Zhang and L. Chang, *Nucl. Phys.* **B291** (1987) 392.
- [20] Z. Bern, L. Dixon, D.A. Kosower and S. Weinzierl, *Nucl. Phys.* **B489** (1997) 3 [hep-ph/9610370].

- [21] W.T. Giele and E.W.N. Glover, *Phys. Rev.* **D46** (1992) 1980.
- [22] Z. Bern, L. Dixon and D.A. Kosower, *Nucl. Phys.* **B513** (1998) 3 [hep-ph/9708239].
- [23] K. Hagiwara, K. Hikasa and N. Kai, *Phys. Rev. Lett.* **52** (1984) 1076.
- [24] L. Dixon, in *QCD & Beyond: Proceedings of TASI '95*, ed. D.E. Soper (World Scientific, 1996) [hep-ph/9601359];  
Z. Bern, L. Dixon and D.A. Kosower, *Ann. Rev. Nucl. Part. Sci.* **46** (1996) 109.
- [25] Z. Bern, L. Dixon and D.A. Kosower, *Nucl. Phys.* **B437** (1995) 259 [hep-ph/9409393].
- [26] W. Siegel, *Phys. Lett.* **84B** (1979) 193;  
D.M. Capper, D.R.T. Jones and P. van Nieuwenhuizen, *Nucl. Phys.* **B167** (1980) 479;  
L.V. Avdeev and A.A. Vladimirov, *Nucl. Phys.* **B219** (1983) 262.
- [27] Z. Bern and D.A. Kosower, *Phys. Rev. Lett.* **66** (1991) 1669;  
Z. Bern and D.A. Kosower, *Nucl. Phys.* **B379** (1992) 451.
- [28] Z. Kunszt, A. Signer and Z. Trócsányi, *Nucl. Phys.* **B411** (1994) 397 [hep-ph/9305239];  
A. Signer, Ph.D. thesis, ETH Zürich (1995);  
S. Catani, M.H. Seymour and Z. Trócsányi, *Phys. Rev.* **D55** (1997) 6819 [hep-ph/9610553].
- [29] K.J. Abraham and B. Lampe, *Nucl. Phys.* **B478** (1996) 507 [hep-ph/9603270].